*Int. J. Solids Structures*, 1972, Vol. 8, pp. 93 to 109. Pergamon Press. Printed in Great Britain

# THE TORSION PROBLEM OF A DISK BONDED TO A DISSIMILAR SHAFT†

F. ERDOGAN and G. D. GUPTA

Department of Mechanical Engineering and Mechanics, Lehigh University, Bethlehem, Pennsylvania

**Abstract**—The torsion of an infinitely long elastic shaft bonded to an elastic disk of finite width and of different elastic constants is considered. The contact may be accomplished through bonding or shrink-fit. First the general problem with the axisymmetric edge cracks on the contact area is formulated. This problem is shown to reduce to a singular integral equation with a simple Cauchy-type singularity. In limit, when the contact is along the entire width of the disk, it is shown that the dominant kernel of the integral equation is of generalized Cauchy-type and the solution has a singularity of the form $(c^2-x^2)^{-\gamma}$, where $2c$ is the width of the disk and $0 < \gamma < \frac{1}{2}$. A series of numerical examples is worked out with or without the edge cracks and under symmetric and anti-symmetric external loads. A variation of the torsion problem, namely, the problem of two semi-infinite strips under anti-plane shear loading is then considered. Again, the results of a series of numerical examples are given to show the effect of the geometry and the material properties on the stress intensity factor.

## 1. INTRODUCTION

IN THIS paper we consider the problem of load transfer from an elastic shaft to an elastic circular disk (Fig. 1). The external loads are assumed to be torques, circumferential body forces, or circumferential tractions applied to the disk and the shaft in an axially symmetric manner. That is, the problem is one of torsion. The outer radius of the disk and the length of the shaft are sufficiently large in comparison with the radius of the shaft and the thickness of the disk so that, in formulating the problem it will be assumed that these dimensions are infinite. The contact between the disk and the shaft may be accomplished through shrink fit or bonding. In either case only the torsion problem under the condition of perfect adhesion will be considered.

The special case of infinitely wide disk was considered in Ref. [1]. In this paper first it will be assumed that the thickness of the disk $2b$ is greater than the length $2c$ of the contact area in $x$ direction (Fig. 1). The configuration without the edge notches, i.e. the case of $b = c$, will then be considered. In presenting the numerical results the emphasis will be on the evaluation of the stress concentration as a function of the relative dimensions, $b/c$ and $a/c$, and the modulus ratio $\mu_2/\mu_1$, where $a$ is the radius of the shaft and $\mu_1$ and $\mu_2$ are, respectively, the shear moduli of the shaft and the disk. The problem will be solved under symmetric and anti-symmetric loading conditions. In the former case $p(x) = p(-x)$ and in the latter $p(x) = -p(-x)$, where $p(x) = \tau_{r\theta}(a, x)$ is the contact stress. The solution under a more general axisymmetric (torsional) loading may be obtained as a proper superposition of these two solutions.

In the special case of infinite shaft radius the problem reduces to one of anti-plane shear. The solution of this problem will be given under the more general condition that the

† This work was supported by the National Science Foundation under Grant GK-11977.

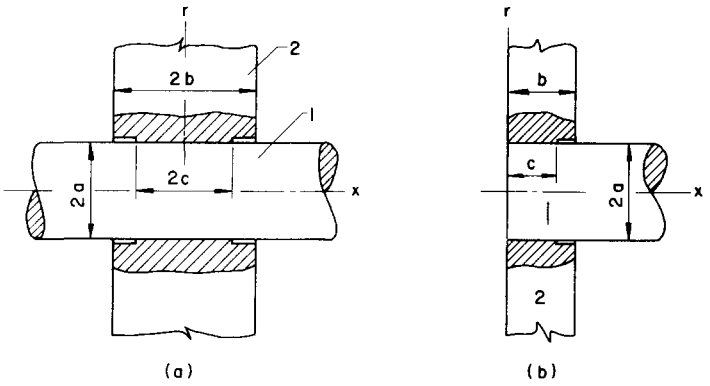


FIG. 1. The geometry of the circular shaft bonded or shrink-fit to a disk.

thicknesses of both materials are finite (Fig. 2). It should be pointed out that in both problems, since under the symmetric loading $x = 0$ is a plane of symmetry on which the traction $\tau_{i\theta z}$ $(i = 1, 2)$ vanishes, the symmetric solution given in this paper is valid also for one half of the composite media shown in Figs. 1(a) and 2 [see, for example, Fig. 1(b)].

## 2. DERIVATION OF THE INTEGRAL EQUATIONS

Consider an infinitely long shaft of radius $a$ and shear modulus $\mu_1$ bonded or shrink-fit to an infinite disk of width $2b$ and shear modulus $\mu_2$ (Fig. 1). Let the axial length of the contact area be $2c$ where $c \leq b$. Let all the external loads act in $\theta$-direction and be distributed in an axially symmetric manner. Thus, the problem is one of torsion and the $\theta$-components $u_1(r, x)$ and $u_2(r, x)$ of the displacement vectors in the shaft and the disk,

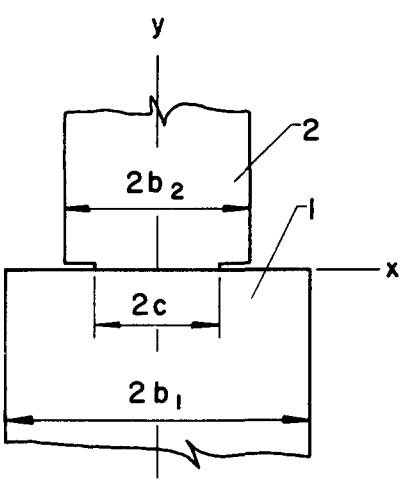


FIG. 2. Bonded semi-infinite strips under anti-plane shear loading.

respectively, are the only unknown functions, which satisfy the following differential equation:

$$\frac{\partial^2 u_i}{\partial r^2}+\frac{1}{r}\frac{\partial u_i}{\partial r}-\frac{u_i}{r^2}+\frac{\partial^2 u_i}{\partial x^2}=0, \qquad (i=1, r<a; i=2, r>a). \tag{1}$$

It will be assumed that the torsion problems for the disk and the shaft have been separately solved under the external loads applied to the disk and the shaft by ignoring the adhesion between the two materials. Let $u_i^0(r, x), (i=1, 2)$ be the displacements corresponding to these solutions, and let

$$f(x) = -\frac{\partial}{\partial x}[u_2^0(a+0, x)-u_1^0(a-0, x)], \qquad (-c<x<c). \tag{2}$$

The final solution will then be $u_i^0+u_i$, $(i=1, 2)$ where $u_1$ and $u_2$ are the displacements obtained from (1) under the following boundary and continuity conditions:

$$\frac{\partial}{\partial x}[u_2(a+0, x)-u_1(a-0, x)] = f(x), \qquad (-c<x<c) \tag{3}$$

$$\tau_{1r\theta}(a, x) = \tau_{2r\theta}(a, x) = p(x), \qquad (-c<x<c) \tag{4}$$

$$\tau_{1r\theta}(a, x) = 0, \qquad |x|>c \tag{5}$$

$$\tau_{2r\theta}(a, x) = 0, \qquad c<|x|<b \tag{6}$$

$$\tau_{2\theta x}(r, \mp b) = 0, \qquad (r>a) \tag{7}$$

$$\int_{-c}^{c} 2\pi a^2 p(x)\,dx = C. \tag{8}$$

Here $p(x)$ is the (unknown) interface shear stress and $C$ is the torque transmitted from the shaft to the disk. The two nonvanishing components of the stress vector are given by

$$\tau_{ir\theta} = \mu_i\left(\frac{\partial u_i}{\partial r}-\frac{u_i}{r}\right), \qquad \tau_{i\theta x} = \mu_i\frac{\partial u_i}{\partial x}, \qquad (i=1, 2). \tag{9}$$

Since $x=0$ is a plane of geometric symmetry, by writing

$$\begin{gathered} f(x) = f_1(x)+f_2(x) \\ f_1(x) = [f(x)-f(-x)]/2, \qquad f_2(x) = [f(x)+f(-x)]/2. \end{gathered} \tag{10}$$

The solution can be expressed as the sum of a symmetric solution, $u_i(r, x) = u_i(r, -x)$, $(i=1, 2)$, $p(x) = p(-x)$ obtained from (1)–(9) by using the input $f_1(x)$ and $C$, and an antisymmetric solution, $u_i(r, x) = -u_i(r, -x)$, $(i=1, 2)$, $p(x) = -p(-x)$ obtained from the input function $f_2(t)$.

The solution of (1) for the shaft and the disk satisfying the conditions of regularity at $r=0$ and $r=\infty$, respectively, may be expressed as

$$u_1(r, x) = \frac{2}{\pi}\int_0^\infty A(\alpha) I_1(\alpha r)\begin{matrix}\cos\\ \sin\end{matrix}(\alpha x)\,d\alpha \tag{11}$$

$$u_2(r, x) = \sum_1^\infty B_n K_1(\alpha_n r)\begin{matrix}\cos\\ \sin\end{matrix}(\alpha_n x) \tag{12}$$

where the function $A(\alpha)$ and the constants $B_n$ are unknown and the cosine and sine kernels correspond to the symmetric and the anti-symmetric problems, respectively. From (7), (9) and (12) we find

$$\alpha_n = \begin{cases} \pi n/b, \text{ (symmetric problem)}, & (n = 1, 2, \ldots) \\ (2n-1)\pi/2b \text{ (anti-symmetric problem)}, & (n = 1, 2, \ldots). \end{cases} \tag{13}$$

From (11), (12) and (9), the boundary conditions (3)–(6) may now be expressed as

$$\lim_{r\to a+0} \sum_1^\infty B_n\alpha_n K_1(\alpha_n r)\begin{Bmatrix} -\sin\alpha_n x \\ \cos\alpha_n x \end{Bmatrix} - \lim_{r\to a-0} \frac{2}{\pi}\int_0^\infty A(\alpha)\alpha I_1(\alpha r)\begin{Bmatrix} -\sin\alpha x \\ \cos\alpha x \end{Bmatrix} d\alpha$$

$$= \begin{cases} f_1(x) \\ f_2(x) \end{cases} \qquad (|x| < c) \tag{14}$$

$$\frac{2\mu_1}{\pi}\int_0^\infty A(\alpha)\alpha I_2(\alpha a)\begin{Bmatrix} \cos\alpha x \\ \sin\alpha x \end{Bmatrix} d\alpha = -\mu_2 \sum_1^\infty B_n\alpha_n K_2(\alpha_n a)\begin{Bmatrix} \cos\alpha_n x \\ \sin\alpha_n x \end{Bmatrix}$$

$$= p(x), \qquad (|x| < c) \tag{15}$$

$$\frac{2\mu_1}{\pi}\int_0^\infty A(\alpha)\alpha I_2(\alpha a)\begin{Bmatrix} \cos\alpha x \\ \sin\alpha x \end{Bmatrix} d\alpha = 0, \qquad (|x| > c) \tag{16}$$

$$-\mu_2 \sum_1^\infty B_n\alpha_n K_2(\alpha_n a)\begin{Bmatrix} \cos\alpha_n x \\ \sin\alpha_n x \end{Bmatrix} = 0, \qquad (c < |x| < b). \tag{17}$$

The dual series-integral equations (14)–(17) may easily be reduced to a singular integral equation for the unknown function $p(x)$ as follows: first from (15)–(17) we obtain

$$\alpha A(\alpha) = \frac{1}{\mu_1 I_2(\alpha a)}\int_0^c p(t)\begin{Bmatrix} \cos\alpha t \\ \sin\alpha t \end{Bmatrix} dt$$

$$\alpha_n B_n = -\frac{2}{b\mu_2 K_2(\alpha_n a)}\int_0^c p(t)\begin{Bmatrix} \cos\alpha_n t \\ \sin\alpha_n t \end{Bmatrix} dt. \tag{18}$$

Then, substituting (18) into (14) and using the symmetry property of $p(t)$ we find

$$\lim_{r\to a+0} \frac{1}{b\mu_2}\int_{-c}^c p(t)\,dt \sum_1^\infty \frac{K_1(\alpha_n r)}{K_2(\alpha_n a)} \sin\alpha_n(t-x) + \lim_{r\to a-0} \frac{1}{\pi\mu_1}\int_{-c}^c p(t)\,dt \int_0^\infty \frac{I_1(\alpha r)}{I_2(\alpha a)} \sin\alpha(t-x)\,d\alpha$$

$$= \begin{cases} -f_1(x) \\ -f_2(x) \end{cases} \qquad (|x| < c). \tag{19}$$

Equation (13) is still valid for $\alpha_n$ appearing in (19). Note that for $b \to \infty$, $1/b \to d\alpha/\pi$ and the kernel in the first term of (19) reduces to that found in Ref. [1].

For $t = x$ the kernels in (19) are divergent. To separate these singular parts of the kernels we let $r = a+\varepsilon$ in the first term and $r = a-\varepsilon$ in the second term of (19), where $\varepsilon$ is a small positive constant and note that for large values of $\alpha$ and $\alpha_n$

$$\frac{K_1(\alpha_n a + \alpha_n\varepsilon)}{K_2(\alpha_n a)} \simeq e^{-\alpha_n\varepsilon}, \quad \frac{I_1(\alpha a - \alpha\varepsilon)}{I_2(\alpha a)} = e^{-\alpha\varepsilon}. \tag{20}$$

We now add and subtract (20) to the integrands in (19) and use the following relations to evaluate the singular kernels [2, 3]

$$\lim_{\varepsilon\to 0}\int_{-c}^{c} p(t)\,dt\int_0^\infty e^{-\alpha\varepsilon}\sin\alpha(t-x)\,d\alpha=\int_{-c}^{c}\frac{p(t)}{t-x}dt$$
$$\sum_1^\infty e^{-\beta n}\sin\lambda n=\frac{\sin\lambda}{2(\operatorname{ch}\beta-\cos\lambda)}. \tag{21}$$

Making use of (21), (19) may be expressed as

$$\frac{1}{\pi}\int_{-c}^{c}\frac{p(t)}{t-x}dt+\frac{\mu_1}{2b\mu_2}\int_{-c}^{c}p(t)\begin{Bmatrix}\cot\dfrac{\pi}{2b}(t-x)\\ \operatorname{cosec}\dfrac{\pi}{2b}(t-x)\end{Bmatrix}dt+\int_{-c}^{c}p(t)k(t,x)\,dt$$
$$=\begin{cases}-\mu_1 f_1(x)\\ -\mu_1 f_2(x)\end{cases},\qquad (|x|<c) \tag{22}$$

$$k(t,x)=\frac{1}{\pi}\int_0^\infty\left(\frac{I_1(\alpha a)}{I_2(\alpha a)}-1\right)\sin\alpha(t-x)\,d\alpha$$
$$+\frac{\mu_1}{b\mu_2}\sum_1^\infty\left(\frac{K_1(\alpha_n a)}{K_2(\alpha_n a)}-1\right)\sin\alpha_n(t-x). \tag{23}$$

The kernel given by (23) is bounded for all values of $t$ and $x$ in $(-c, c)$ where, because of uniform convergence, the limit can be (and is) put under the integral and summation signs.

For $b > c$ the kernel in the second term of (22) has a singularity of the form $1/(t-x)$, and hence (22) is a simple singular integral equation. In this case the function $p(t)$ has an integrable singularity at $\mp c$ of the form $(c^2-t^2)^{-1/2}$. The case of $b = c$ will be discussed in Section 4. In either case, (22) must be solved subject to the condition (8).

## 3. INTEGRAL EQUATION FOR BONDED STRIPS

The formulation given in the previous section may be used to derive the integral equation for the anti-plane shear problem of two bonded semi-infinite strips shown in Fig. 2. For $a\to\infty$ the Fredholm kernel, $k(x, t)$ given by (23) vanishes, and (22) gives the integral equation for a strip bonded to a half plane. If the width of the medium 1 is also finite, (22) may easily be modified as follows:

$$\frac{1}{2b_1\mu_1}\int_{-c}^{c}p(t)\begin{Bmatrix}\cot\dfrac{\pi}{2b_1}(t-x)\\ \operatorname{cosec}\dfrac{\pi}{2b_1}(t-x)\end{Bmatrix}dt+\frac{1}{2b_2\mu_2}\int_{-c}^{c}p(t)\begin{Bmatrix}\cot\dfrac{\pi}{2b_2}(t-x)\\ \operatorname{cosec}\dfrac{\pi}{2b_2}(t-x)\end{Bmatrix}dt$$
$$=\begin{cases}-f_1(x)\\ -f_2(x)\end{cases}\qquad (|x|<c) \tag{24}$$

where, again, the upper and lower kernels and the right-hand side correspond to symmetric and anti-symmetric problems, respectively. For $b_1 > c$, $b_2 > c$, the kernel of (24) has a Cauchy-type singularity. The special cases of $b_1 = c < b_2$ and $b_1 = c = b_2$ will be discussed in the next section. The integral equation (24) will be solved subject to the following condition

$$\int_{-c}^{c} p(t)\,dt = P \tag{25}$$

where $P$ is the resultant anti-plane shear load per unit thickness in $z$-direction (Fig. 2).

## 4. THE CASE OF $b = c$

Referring to Fig. 1, if there are no edge cracks on the interface, that is, if $b = c$, the kernels in the second term of (22) become unbounded at $t-x = \mp 2c$, as well as at $t = x$. Thus, separating the singular parts, these kernels may be expressed as

$$\begin{aligned}
&\frac{1}{2c}\cot\frac{\pi}{2c}(t-x) = \frac{1}{\pi}\left(\frac{1}{t-x}+\frac{1}{t-z_1}+\frac{1}{t-z_2}\right)+k_1(x,t),\\
&\frac{1}{2c}\operatorname{cosec}\frac{\pi}{2c}(t-x) = \frac{1}{\pi}\left(\frac{1}{t-x}-\frac{1}{t-z_1}-\frac{1}{t-z_2}\right)+k_2(x,t),\\
&z_1 = x-2c, \qquad z_2 = x+2c, \quad -3c < z_1 < -c, \; c < z_2 < 3c,
\end{aligned} \tag{26}$$

where $k_1$ and $k_2$ are bounded in the closed interval $[-c, c]$. Substituting from (26) into (22), the integral equation for the symmetric problem becomes

$$\frac{1}{\pi}\int_{-c}^{c} p(t)\left(\frac{1}{t-x}+\frac{\lambda}{t-z_1}+\frac{\lambda}{t-z_2}\right)dt = F(x), \qquad (-c < x < c) \tag{27}$$

where

$$\lambda = \mu_1/(\mu_1+\mu_2)$$

$$F(x) = -\lambda\mu_2 f_1(x) - \lambda\int_{-c}^{c}\left[\frac{\mu_2}{\mu_1}k(x,t)+k_1(x,t)\right]p(t)\,dt.$$

Since $k$ and $k_1$ are bounded and $p$ is integrable, $F(x)$ is a bounded function in the closed interval $[-c, c]$.

We will now assume that $p(t)$ has an integrable singularity at $t = \mp c$, and can be expressed as follows [4, chapter 4]:

$$p(t) = \frac{g(t)}{(c^2-t^2)^{\gamma}} = \frac{g(t)\,e^{\pi i\gamma}}{(t-c)^{\gamma}(t+c)^{\gamma}}, \qquad (|t| < c) \tag{28}$$

where $\gamma = \alpha+i\beta$, $0 < \alpha < 1$, $g(t)$ satisfies a Hölder condition in the closed interval $-c \le t \le c$, and $(t^2-c^2)^{\gamma}$ is any definite branch which varies continuously on $-c < t < c$. Consider the following sectionally holomorphic function

$$\phi(z) = \frac{1}{\pi}\int_{-c}^{c}\frac{p(t)}{t-z}\,dt = \frac{1}{\pi}\int_{-c}^{c}\frac{g(t)\,e^{\pi i\gamma}\,dt}{(t-c)^{\gamma}(t+c)^{\gamma}(t-z)}. \tag{29}$$

Following [4, chapter 4], after examining the singular behavior of $\phi(z)$ near the end points $\mp c$ it may be expressed as

$$\phi(z) = \frac{g(-c)}{(2c)^\gamma}\frac{e^{\pi i\gamma}}{\sin\pi\gamma}\frac{1}{(z+c)^\gamma} - \frac{g(c)}{(2c)^\gamma\sin\pi\gamma}\frac{1}{(z-c)^\gamma} + \phi_0(z). \tag{30}$$

The function $\phi_0(z)$ is bounded everywhere with the exception of the end points $\mp c$ near which it has the following behavior:

$$|\phi_0(z)| < \frac{C_k}{|z-c_k|^{\alpha_0}}, \qquad k = 1, 2, \qquad \alpha_0 < \alpha, \qquad c_k = \mp c \tag{31}$$

where $C_k$ and $\alpha_0$ are real constants. In particular, for $z = x$, $-c < x < c$ we have [4]

$$\phi(x) = \frac{1}{\pi}\int_{-c}^{c}\frac{p(t)\,dt}{t-x} = \frac{g(-c)}{(2c)^\gamma}\frac{\cot\pi\gamma}{(x+c)^\gamma} - \frac{g(c)}{(2c)^\gamma}\frac{e^{\pi i\gamma}\cot\pi\gamma}{(x-c)^\gamma} + \phi^*(x), \ (-c < x < c). \tag{32}$$

Near the end points $\phi^*(x)$ behaves as

$$\phi^*(x) = \frac{\phi_k^{**}(x)}{|x-c_k|^{\alpha_0}}, \qquad (k = 1, 2), \qquad \alpha_0 < \alpha, \qquad c_k = \mp c \tag{33}$$

where $\phi_k^{**}(x)$, $(k = 1, 2)$ satisfies a Hölder condition near and at the ends $x = \mp c$.

Note that the points $z_1$ and $z_2$ are outside the cut $-c < x < c$. Hence at $z_1$ and $z_2$ $\phi(z)$ is holomorphic and may be expressed as

$$\phi(z_1) = \frac{g(-c)}{(2c)^\gamma}\frac{e^{\pi i\gamma}}{\sin\pi\gamma}\frac{1}{(z_1+c)^\gamma} + \phi_1(z_1)$$

$$= \frac{g(-c)}{(2c)^\gamma}\frac{1}{\sin\pi\gamma}\frac{1}{(c-x)^\gamma} + \phi_1(x-2c). \tag{34}$$

$$\phi(z_2) = -\frac{g(c)}{(2c)^\gamma}\frac{1}{\sin\pi\gamma}\frac{1}{(z_2-c)^\gamma} + \phi_2(z_2)$$

$$= -\frac{g(c)}{(2c)^\gamma}\frac{1}{\sin\pi\gamma}\frac{1}{(c+x)^\gamma} + \phi_2(x+2c). \tag{35}$$

The behavior of $\phi_1$ near $z_1 = -c$ and that of $\phi_2$ near $z_2 = c$ are given by (31), elsewhere on the cut $\phi_1$ and $\phi_2$ are bounded.

Substituting from (29), (32), (34) and (35) into (27) we obtain

$$\frac{g(-c)}{(2c)^\gamma}\frac{\cot\pi\gamma}{(c+x)^\gamma} - \frac{g(c)}{(2c)^\gamma}\frac{\cot\pi\gamma}{(c-x)^\gamma} + \phi^*(x) + \lambda\frac{g(-c)}{(2c)^\gamma}\frac{1}{\sin\pi\gamma}\frac{1}{(c-x)^\gamma} + \lambda\phi_1(x-2c)$$

$$-\lambda\frac{g(c)}{(2c)^\gamma}\frac{1}{\sin\pi\gamma}\frac{1}{(c+x)^\gamma} + \lambda\phi_2(x+2c) = F(x), \qquad (|x| < c). \tag{36}$$

Here, we recall that (27) was expressed for the symmetric problem, that is, $p(t) = p(-t)$ or $g(t) = g(-t)$. Using this symmetry property and noting that $g(t) \neq 0$ at $t = \mp c$, from

(36) first by multiplying through $(c+x)^{\gamma}$ and substituting $x = -c$, and then by multiplying through $(c-x)^{\gamma}$ and substituting $x = c$ we find

$$\frac{g(c)}{(2c)^{\gamma}}\left(\cot \pi\gamma - \frac{\lambda}{\sin \pi\gamma}\right) = 0$$

or

$$\cos \pi\gamma = \lambda. \tag{37}$$

From (37) it is seen that the power of the singularity, $\gamma$ is a real constant. The range of $\lambda$ is $0 < \lambda = \mu_1/(\mu_1+\mu_2) < 1$, giving $0 < \gamma < \frac{1}{2}$. The well-known limiting cases are $\gamma = \frac{1}{2}$ for $(\mu_2/\mu_1) = \infty$, and $\gamma = 0$ for $(\mu_2/\mu_1) = 0$.

In the anti-symmetric problem, from (22) and (26) it follows that on the left-hand side of (27) and (36) the sign of $\lambda$ will be negative and the right-hand side will be replaced by another bounded function. However, in this case $p(t) = -p(-t)$ or $g(c) = -g(-c)$, giving again (37) as the characteristic equation for $\gamma$.

In the bonded strips (Fig. 2), the comparison of (24) and (22) indicates that for $b_1 > c$, $b_2 = c$ the dominant part of (27) remains unchanged; hence, (37) is still valid. In addition to $b_2 = c$ if we also let $b_1 = c$, from (24) and (26) we find

$$\left(\frac{1}{\mu_1}+\frac{1}{\mu_2}\right)\frac{1}{\pi}\int_{-c}^{c} p(t)\left(\frac{1}{t-x}\pm\frac{1}{t-z_1}\pm\frac{1}{t-z_2}\right)\mathrm{d}t = \begin{cases} F_1(x) \\ F_2(x) \end{cases} \qquad (|x| < 1) \tag{38}$$

where $F_1$ and $F_2$ are bounded in the closed interval $|x| \le c$. Thus, from (27), (38) and (37) it is seen that, in this case $\cos \pi\gamma = 1$, or $\gamma = 0$, meaning that at $x = \mp c$, $y = 0$ the stresses are bounded.

If $b > c$ in Fig. 1 and (22), and $b_1 > c$, $b_2 > c$ in Fig. 2 and (24), the only singular parts of the cotangent and cosecant kernels will be $1/\pi(t-x)$. As a result, both in the symmetric and in the anti-symmetric problem the dominant part of the integral equation (27) will have only the simple Cauchy kernel $1/(t-x)$. In this case, following the analysis (27)–(37), instead of (37) we obtain the characteristic equation giving $\gamma$ as

$$\cot \pi\gamma = 0, \gamma = \tfrac{1}{2} \tag{39}$$

which is the well-known result [5].

## 5. SOLUTION OF THE INTEGRAL EQUATIONS

To solve the integral equations (22) and (24), we will first normalize the dimensions with respect to $c$ by introducing the following quantities:

$$\begin{aligned} &\tau = t/c, \quad \xi = x/c, \quad u = \alpha c, \quad u_n = \alpha_n c, \quad v_n = \beta_n c, \\ &a_0 = a/c, \quad b_0 = b/c, \quad b_{10} = b_1/c, \quad b_{20} = b_2/c, \\ &p(t) = p(c\tau) = \phi(\tau), \quad f_j(x) = s_j(\xi), \quad (j = 1, 2). \end{aligned} \tag{40}$$

Thus, for the symmetric problem, and for $b > c$ (22) may be expressed as

$$\frac{1}{\pi}\int_{-1}^{1}\frac{\phi(\tau)\,\mathrm{d}\tau}{\tau-\xi}+\int_{-1}^{1} h(\xi,\tau)\phi(\tau)\,\mathrm{d}\tau = -\mu_2\lambda s_1(\xi), \qquad (|\xi| < 1) \tag{41}$$

where

$$h(\xi,\tau)=\lambda\left[\frac{1}{2b_0}\cot\frac{\pi}{2b_0}(\tau-\xi)-\frac{1}{\pi}\frac{1}{\tau-\xi}\right]+\frac{c\mu_2}{\mu_1+\mu_2}k(c\tau,c\xi)$$

$$\lambda=\mu_1/(\mu_1+\mu_2).$$

Equation (41) will be solved subject to the equilibrium condition (8) which becomes

$$2\pi a_0^2c^3\int_{-1}^{1}\phi(\tau)\,d\tau=C. \tag{42}$$

To obtain the solution of (41) we will use the method described in [6]. The method is based on the following Gauss–Chebyshev integration formula for singular integrals developed in [6]:

$$\frac{1}{\pi}\int_{-1}^{1}\frac{G(\tau)\,d\tau}{(\tau-\xi_r)(1-\tau^2)^{1/2}}\simeq\sum_{k=1}^{n}\frac{G(\tau_k)}{n(\tau_k-\xi_r)},\qquad(|\xi_r|<1) \tag{43}$$

where $G(\tau)$ satisfies a Hölder condition in the closed interval $-1\le\tau\le1$, and $\tau_k$ and $\xi_r$ are the roots of appropriate Chebyshev polynomials given by

$$\begin{aligned}&T_n(\tau_k)=0,\qquad \tau_k=\cos\frac{\pi}{2n}(2k-1),\qquad(k=1,\ldots,n)\\&U_{n-1}(\xi_r)=0,\qquad \xi_r=\cos\frac{\pi r}{n},\qquad(r=1,\ldots,n-1).\end{aligned} \tag{44}$$

Expressing now the solution of (41) as [see, (28) and (39)]

$$\phi(\tau)=\frac{G(\tau)}{(1-\tau^2)^{\frac{1}{2}}} \tag{45}$$

and using the ordinary Gauss–Chebyshev integration formula [7, 8]

$$\frac{1}{\pi}\int_{-1}^{1}\frac{f(\tau,\xi)\,d\tau}{(1-\tau^2)^{\frac{1}{2}}}\simeq\sum_{1}^{n}\frac{f(\tau_k,\xi)}{n},\qquad T_n(\tau_k)=0 \tag{46}$$

to evaluate the second integral in (41), we obtain

$$\sum_{k=1}^{n}\frac{1}{n}G(\tau_k)\left[\frac{1}{\tau_k-\xi_r}+\pi h(\xi_r,\tau_k)\right]\simeq-\mu_2\lambda s_1(\xi_r),\qquad(r=1,\ldots,n-1). \tag{47}$$

Equation (47) provides $(n-1)$ linear algebraic equations for the unknowns $G(\tau_1),\ldots,G(\tau_n)$. The $n$th equation is obtained from (42) which can be written as

$$2\pi^2a_0^2c^3\sum_{k=1}^{n}\frac{1}{n}G(\tau_k)=C. \tag{48}$$

After evaluating $G(\tau)$, the interface shear stress $p(t)$ and the stress intensity factor $k$ may be obtained from

$$\begin{aligned}p(t)&=\frac{cG(t/c)}{(c^2-t^2)^{\frac{1}{2}}},\qquad(-c<t<c)\\k&=\lim_{t\to c}[2(c-t)]^{\frac{1}{2}}p(t)=c^{\frac{1}{2}}G(1).\end{aligned} \tag{49}$$

In solving the anti-symmetric problem the only change will be in the expression of the Fredholm kernel, $h(\xi, \tau)$ and the right-hand side of (41), otherwise, the procedure remains the same. The development of the Gauss–Chebyshev integration formula for singular integrals, (43), is based on the fact that the fundamental solution, $w(t) = (1-\tau^2)^{-\frac{1}{2}}$, of the dominant part of the integral equation is the weight function of the Chebyshev polynomials $T_n(\tau)$. Thus, if the bounded function can be expressed as

$$G(\tau) = \sum_0^p B_j T_j(\tau), \qquad p < n, \qquad (-1 < \tau < 1) \tag{50}$$

it can be proved that [6] the integration formula is exact for values of $\xi = \xi_r$, $U_{n-1}(\xi_r) = 0$.

For $b = c$, the dominant part of the singular integral equation is shown in (27). In terms of dimensionless variables defined by (40) the fundamental solution of the integral equation is [see (28) and (37)]

$$w(\tau) = (1-\tau^2)^{-\gamma}, \qquad \cos \pi\gamma = \lambda, \qquad (-1 < \tau < 1). \tag{51}$$

The fundamental solution, $w(\tau)$, given by (51) is the weight function of the Jacobi polynomials $P_n^{(-\gamma,-\gamma)}(\tau)$, of which $\gamma = \frac{1}{2}$ described above is a special case. Hence, the method of solution of (22) will be similar to that of (41) mentioned previously. Since the separation of the dominant part of the singular integral equations [see (27)] serves no specific purpose other than obtaining the characteristic equation and finding the fundamental solution, the method can be applied to the equation in its original form, (22), which in terms of the quantities defined by (40), may be expressed as

$$\frac{1}{\pi}\int_{-1}^{1} \frac{\phi(\tau)\,d\tau}{\tau-\xi} + \frac{\mu_1}{2b_0\mu_2}\int_{-1}^{1} \phi(\tau)\begin{Bmatrix} \cot\dfrac{\pi}{2b_0}(\tau-\xi) \\ \operatorname{cosec}\dfrac{\pi}{2b_0}(\tau-\xi) \end{Bmatrix} d\tau$$

$$+ \int_{-1}^{1} \phi(\tau) k(c\xi, c\tau) c\, d\tau = \begin{cases} -\mu_1 s_1(\xi) \\ -\mu_1 s_2(\xi) \end{cases}, \qquad (-1 < \xi < 1). \tag{52}$$

The basic formula, known as the Gauss–Jacobi integration formula [7, 8], which will be used to solve (52) is

$$\int_{-1}^{1} f(\tau, \xi)(1-\tau)^{-\alpha}(1+\tau)^{-\beta}\, d\tau \simeq \sum_{k=1}^{n} A_k f(\tau_k, \xi), \qquad [0 < (\alpha, \beta) < 1] \tag{53}$$

where $\tau_k$ are the roots of

$$P_n^{(-\alpha,-\beta)}(\tau_k) = 0, \qquad (k = 1, \ldots, n) \tag{54}$$

and the weighting constants are given by

$$A_k = -\frac{2n-\alpha-\beta+2}{(n+1)!(n-\alpha-\beta+1)} \frac{\Gamma(n-\alpha+1)\Gamma(n-\beta+1)}{\Gamma(n-\alpha-\beta+1)} \frac{2^{-\alpha-\beta}}{P_n'^{(-\alpha,-\beta)}(\tau_k) P_{n+1}^{(-\alpha,-\beta)}(\tau_k)}. \tag{55}$$

Thus, defining

$$\phi(\tau) = G(\tau)(1-\tau^2)^{-\gamma}, |\tau| < 1 \tag{56}$$

and using (53), (52) may be expressed as

$$\sum_{j=1}^{n} A_j G(\tau_j)\left[\frac{1}{\pi(\tau_j-\xi_r)}+\frac{\mu_1}{2\mu_2 b_0}\begin{Bmatrix}\cot\dfrac{\pi}{2b_0}(\tau_j-\xi_r)\\ \operatorname{cosec}\dfrac{\pi}{2b_0}(\tau_j-\xi_r)\end{Bmatrix}\right.$$

$$\left.+ck(c\xi_r, c\tau_j)\right] = \begin{cases}-\mu_1 s_1(\xi_r)\\ -\mu_1 s_2(\xi_r),\end{cases} \qquad (r = 1,\ldots,n-1) \tag{57}$$

where $\xi_r$ are now the roots of†

$$P_{n-1}^{(1-\gamma,1-\gamma)}(\xi_r) = 0, \qquad (r = 1,\ldots,n-1). \tag{58}$$

Again, (52) is subject to the equilibrium condition (42), which may be written as

$$\sum_{1}^{n} A_k G(\tau_k) = \frac{C}{2\pi a^2 c}. \tag{59}$$

Equations (57) and (59) provide $n$ equations for the unknowns $G(\tau_j), (j = 1,\ldots,n)$.

In this problem too one can define a "stress intensity factor", $k'$ describing the stresses in the close neighborhood of the singular points such that

$$p(x) \simeq \frac{k'}{(2\rho)^\gamma} \tag{60}$$

where $\rho = c-x$ is very small compared to $c$. Thus, from (56), (40) and (60) we obtain

$$\begin{aligned} p(t) &= \frac{c^{2\gamma}G(t/c)}{(c^2-t^2)^\gamma}\\ k' &= \lim_{t\to c}[2(c-t)]^\gamma p(t) = c^\gamma G(1). \end{aligned} \tag{61}$$

After $p(t)$ is determined, (11), (12) and (18) give the complete solution of the problem.

## 6. NUMERICAL RESULTS AND DISCUSSION

The numerical results obtained from the solution of (47) and (57) are shown in Figs. 3–10. In the shaft problem (Fig. 1) the external loads are assumed to be torques applied to the body at sufficient distances away from the contact area, $r = a$, $-c < x < c$, so that the assumptions regarding the axial symmetry and infinite dimensions are justified. In the symmetric problem each side of the shaft is subjected to a torque, $C/2$. Thus, in this case the input function $f_1(x)$ is zero [see, (3) and (10), and the insert in Fig. 3]. In the anti-symmetric problem the external loads are the torques $-C/2$ and $C/2$ applied to opposite ends of the shaft. Hence, the total torque transmitted through the contact area is zero and the equilibrium equations (48) and (59) become homogeneous. In this case, however, the input function $f_2(x)$ defined by (10) and (3) is

$$-\mu_1 f_2(x) = \frac{C}{\pi a^3}. \tag{62}$$

† See [7] for the computer programs giving the roots of (54) and (58). Also see [7, 8] for the error estimates in (53) and (46).

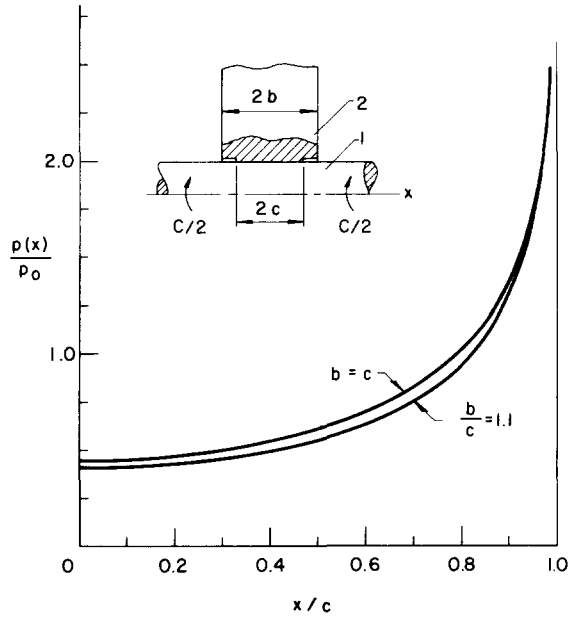


FIG. 3. Contact stress for the shaft under symmetric loading; $\mu_2/\mu_1 = 0{\cdot}345$, $\gamma = 0{\cdot}23317$.

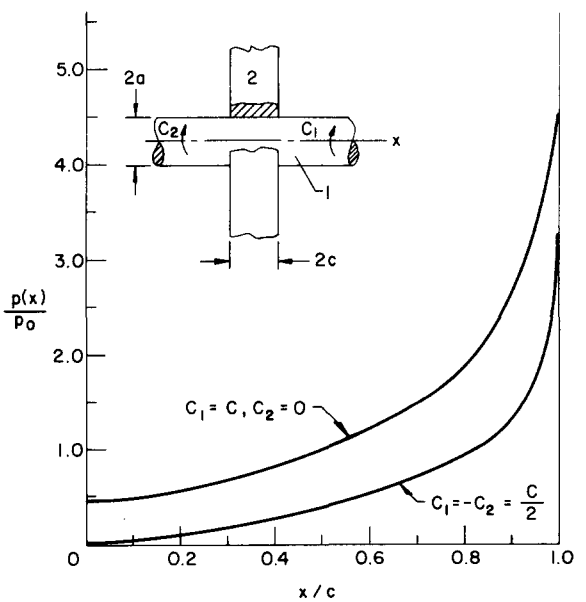


FIG. 4. Contact stress for the shaft under anti-symmetric ($C_1 = -C_2$) and non-symmetric ($C_1 = C, C_2 = 0$) loading; $\mu_2/\mu_1 = 0{\cdot}345$, $\gamma = 0{\cdot}23317$.

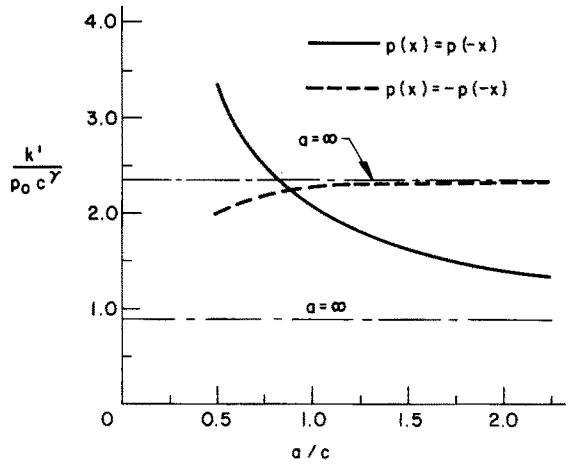


FIG. 5. Stress intensity factor vs. the shaft radius; $b = c$, $\mu_2/\mu_1 = 0{\cdot}345$, $\gamma = 0{\cdot}23317$.

In Figs. 3–6 the results are given in dimensionless form by introducing a normalizing constant stress $p_0$ defined by

$$p_0 = \frac{C}{2\pi^2 a^2 c}. \tag{63}$$

In the anti-plane shear problem of the bonded strips (Figs. 7–10) the normalizing stress is $P/\pi c$, $P$ being the total shear load (per unit thickness in $z$ direction) transmitted through the contact area $y = 0$, $-c < x < c$ (Fig. 2). The choice of these normalizing stresses is based on the fact that in the elementary case of the anti-plane shear loading of two half planes bonded along $y = 0$, $-c < x < c$, the stress intensity factor ratio $k/p_0\sqrt{(c)} = \pi\sqrt{(c)}k/P$ is unity.†

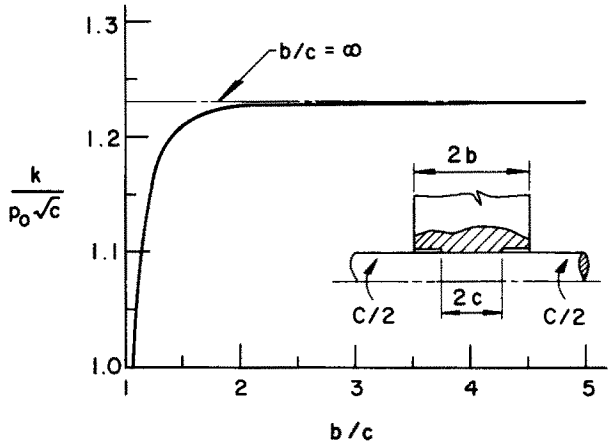


FIG. 6. Stress intensity factor vs. $b/c$; $a/c = 1$, $\mu_2/\mu_1 = 0{\cdot}345$, $\gamma = 0{\cdot}23317$.

† It should be pointed out that $p_0$ is not the average stress on the contact area. The average stress in both cases is $p_{av} = \pi p_0/2$.

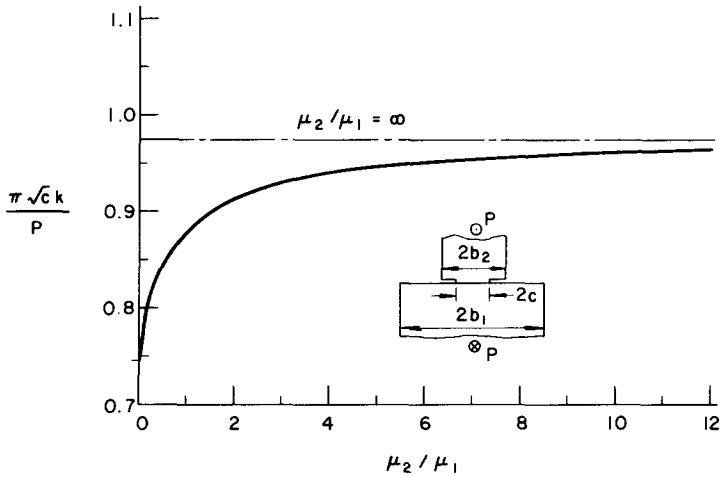


FIG. 7. Stress intensity factor vs. modulus ratio in bonded strips under symmetric anti-plane shear loading; $b_1/c = 5{\cdot}0, b_2/c = 1{\cdot}5$.

Even though in all cases considered the contact stresses were obtained, in presenting the numerical results in this paper the main emphasis will be on the stress intensity factors $k$ and $k'$ [see, (49) and (61)], as they fully describe the stress state around the structurally critical locations, namely, the singular points. However, to give an idea about the distribution of the contact shear, some sample results are shown in Figs. 3 and 4. Figure 3 shows the contact stresses for the shaft subjected to symmetric torques $C/2$. The results are given for $b = c$ and $b = 1{\cdot}1c$, and for $\mu_2/\mu_1 = 0{\cdot}345$. Figure 4 shows the results for the anti-symmetric loading $C_1 = C/2 = -C_2$, and the nonsymmetric loading in which the torque $C$ is applied

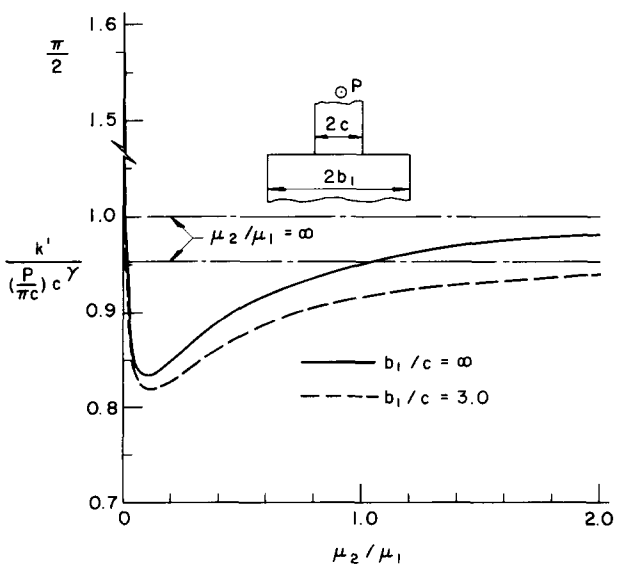


FIG. 8. Stress intensity factor vs. $\mu_2/\mu_1$ in bonded strips under symmetric anti-plane shear loading; $b_2 = c, b_1 > c$.

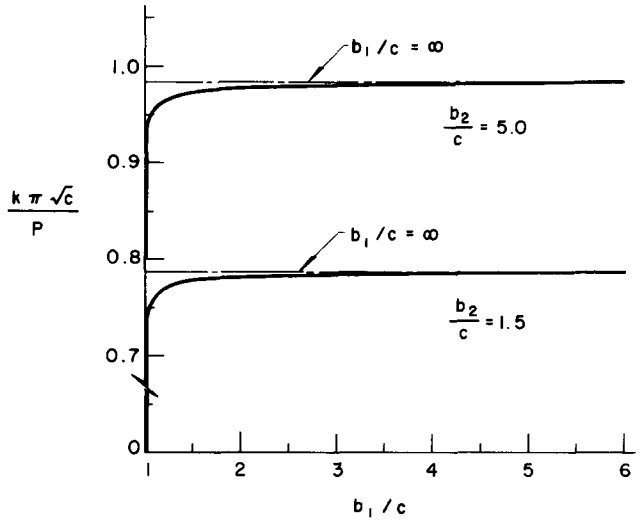


FIG. 9. Stress intensity factor vs. $b_1/c$ in bonded strips under symmetric anti-plane shear loading; $\mu_2/\mu_1 = 1/21{\cdot}7$.

to the shaft on one side only. This last result is obtained through the superposition of the symmetric and anti-symmetric contact stresses given in Figs. 3 and 4.

Figure 5 shows the stress intensity factor ratio $k'/p_0c^\gamma$ as a function of $a/c$ for the symmetric [i.e. $C_1 = C_2 = C/2$, $p(x) = p(-x)$] and for the anti-symmetric [i.e. $C_1 = -C_2 = C/2$, $p(x) = -p(-x)$] problems with $b = c$ and $\mu_2/\mu_1 = 0{\cdot}345$. The figure also shows the asymptotic value for $a/c \to \infty$ obtained from the anti-plane shear problem (see Fig. 8). Note that for constant $c$, $\rho_0 \sim C/a^2$ [see (63)]. Thus, for constant $C$ and $c$, the values on Fig. 5 should be multiplied by $1/a^2$ to obtain $k'$. This means that, even though there is a slight decrease in the stress intensity factor ratio for the anti-symmetric case as $a/c$ decreases, in both cases $k'$ would rapidly increase as $a/c \to 0$.

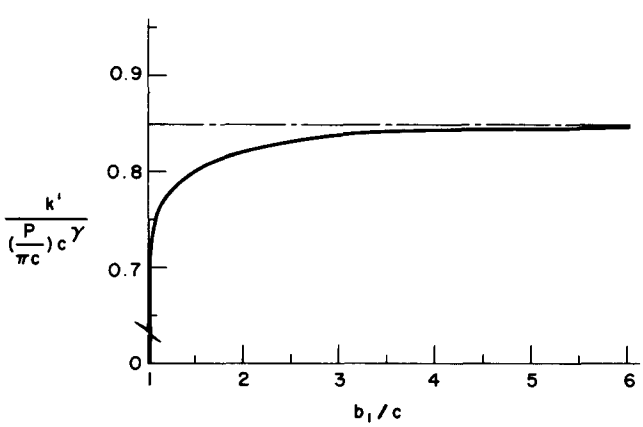


FIG. 10. Stress intensity factor vs. $b_1/c$ in bonded strips under symmetric anti-plane shear loading; $b_2 = c$, $\mu_2/\mu_1 = 1/21{\cdot}7$.

For the symmetric problem in the shaft and for $b > c$, $a/c = 1$ and $\mu_2/\mu_1 = 0{\cdot}345$ the variation of the stress intensity factor ratio $k/p_0\sqrt{(c)}$ with $b/c$ is shown in Fig. 6. It is seen that the stress intensity factor is practically independent of $b/c$ for $b > 2c$. For $b < 2c$, $k$ decreases rather rapidly with decreasing $b$, and in the limiting case of $b = c$, since $p(x) \sim (c^2 - x^2)^{-\gamma}, 0 < \gamma < \frac{1}{2}$ and $k$ is defined by (49) where $\gamma = \frac{1}{2}$, in this graph $k$ will go to zero.

Figure 7 shows the stress intensity factor ratio $k/(P/\pi\sqrt{(c)})$ as a function of $\mu_2/\mu_1$ (Fig. 2) in bonded strips under (symmetric) anti-plane shear loading. For this example the widths of the strips are constant ($b_1/c = 5{\cdot}0$ and $b_2/c = 1{\cdot}5$) and $P$ is the total load applied to the strips in $z$ direction away from the contact area. In this case the limiting values of $k$ for $\mu_2/\mu_1 = \infty$ and $\mu_2/\mu_1 = 0$ are obtained from the closed solution for the infinite strip of width $2b$ with symmetric edge cracks given by [9] †

$$p(x) = \frac{P}{2b}\cos\frac{\pi c}{2b}\Big/\left(\sin^2\frac{\pi c}{2b} - \sin^2\frac{\pi x}{2b}\right)^{\frac{1}{2}}. \tag{64}$$

The results for the limiting case of $b = c$ in the symmetric problem are shown in Fig. 8. Note that $\gamma$ is a function of $\mu_2/\mu_1$, [i.e. $\cos\pi\gamma = 1/(1+\mu_2/\mu_1)$] varying from $\gamma = 0$ for $\mu_2/\mu_1 = 0$ to $\gamma = \frac{1}{2}$ for $\mu_2/\mu_1 = \infty$. The asymptotic values of $k'$ for $\mu_2 = \infty$ are obtained from the closed form solution (64). The solution for $\mu_1 = \infty$ is simply $p(x) = P/2c$. In this case since $\gamma = 0$, this is also the value of $k'$ [see (61)]. Thus, for $\mu_2/\mu_1 \to 0$ the limiting value of $k'/(c^{\gamma}P/\pi c)$ will be $\pi/2$.

Figures 9 and 10 show the variation of the stress intensity factor with $b_1/c$ for $\mu_2/\mu_1 = 1/21{\cdot}7$ and for $b_2/c = 5$, $1{\cdot}5$ and 1. Since for $b_2 > c$ and $b_1 = c$, $p(x) \sim (c^2 - t^2)^{-\gamma'}$, $\cos\gamma' = 1/(1+\mu_1/\mu_2)$, $0 < \gamma' < \frac{1}{2}$, $k$ shown in Fig. 9 will go to zero as $b_1 \to c$. Similarly, since for $b_2 = c = b_1$, $p(x)$ is bounded at $\mp c$, $k'$ shown in Fig. 10 will also go to zero as $b_1 \to c$.

If the contact between the shaft and the disk is accomplished through shrink-fit, in the neighborhood of the singular points a state of plane strain prevails which has to be superimposed on the solution given in this paper. At present, the complete solution of the problem is not available. However, in the plane strain case the contact stresses around the singular point, $x = c$ are known to be of the form [10]

$$\tau_{rr} + i\tau_{rx} \sim \frac{F_1}{(c-x)^{\omega}} + \frac{F_2}{(c-x)^{\bar{\omega}}} \tag{65}$$

where $F_1$ and $F_2$ are bounded and are functions of elastic constants, dimensions and the external loads. The power of the singularity, $\omega$, is a function of the elastic constants only. For the particular case of $\nu_1 = \nu_2 = 0{\cdot}2$, Fig. 11 shows the variation of $\omega$ as well as of $\gamma$ with $\mu_2/\mu_1$ (see [10]). If we assume that the elasticity solution is applicable and there is a constant coefficient of friction between the contacting surfaces, it is clear that partial slip may take place on the contact area as the torque is increased above a certain value which is proportional to the shrink-fit clearance. Figure 11 gives a qualitative idea about the nature of this phenomenon. For $\mu_2/\mu_1 < 9$, since $\omega$ is real and greater than $\gamma$, the possibility of slip initiating at the ends $x = \mp c$ will be small. For $\mu_2/\mu_1 > 10$, $\omega$ is complex, meaning that the plane strain problem has an oscillating singularity. Furthermore, in this range since $\gamma \leq \text{Re}\,\omega$ (again, depending on the torque–clearance ratio), some slip would almost certainly take place near the corners.

† The closed form solution for this problem can also be obtained by using the method given in this paper.

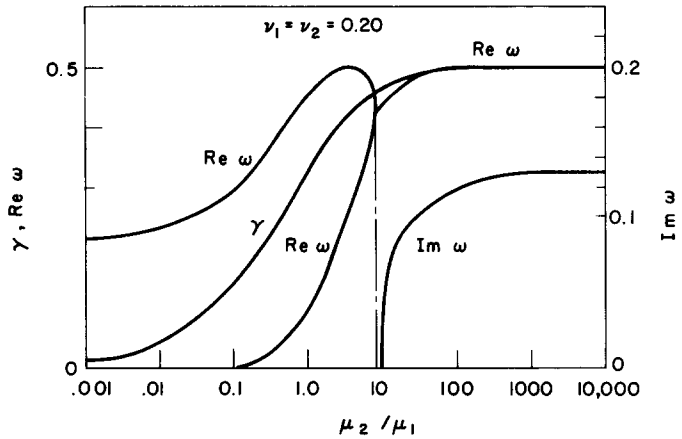


FIG. 11. Variation of the power of singularity in plane strain ($\omega$) and in anti-plane shear ($\gamma$) problems as functions of $\mu_2/\mu_1$.

## REFERENCES

[1] F. ERDOGAN and T. OZBEK, Shrink-fit cylinders under torsion. *J. appl. Mech.* **37**, 233–234 (1970).
[2] F. ERDOGAN, Simultaneous dual integral equations with trigonometric and Bessel kernels. *Z. angew. Math. Mech.* **48**, 217–225 (1968).
[3] I. S. GRADSHTEYN and I. M. RYZHIK, *Table of Integrals Series and Products*. Academic Press (1965).
[4] N. I. MUSKHELISHVILI, *Singular Integral Equations*. P. Noordhoff (1953).
[5] F. ERDOGAN, Elastic–plastic anti-plane problems for bonded dissimilar media containing cracks and cavities. *Int. J. Solids Struct.* **2**, 447–465 (1966).
[6] F. ERDOGAN and G. D. GUPTA, On the numerical solution of singular integral equations, *Q. appl. Math.* to appear.
[7] A. H. STROUD and DON SECREST, *Gaussian Quadrature Formulas*. Prentice-Hall (1966).
[8] A. RALSTON, *A First Course in Numerical Analysis*. McGraw-Hill (1965).
[9] F. ERDOGAN, Elastic–Plastic Anti-Plane Problems in Infinite Planes and Strips with Cracks or Cavities, Technical Report for NASA under Contract NGR-39-007-011 (1966).
[10] V. L. HEIN and F. ERDOGAN, Stress singularities in a two-material wedge. *Int. J. Fracture Mech.* to appear.

(*Received* 18 *May* 1971)

**Абстракт** Исследуется кручение бесконечно длинного упругого вала, присоединенного к упругому диску конечной ширины и с разными упругими постоянными.

Контакт может реализоватся путём присоединения или горячепрессовой посадки. Сначала даётся формула общей задачи для осесимметричесих краевых трещин на площади контакта. Оказывается, что решение сводится к сингулярному интегральному уравнинию, с простой сингулярностью типа Коми.

В предельном случае, когда контакт существует вдоль всей ширины диска, тогда преобладающим ядром интеградьного уравнения является обобщенное ядро типа Коми. Решение имеет сингулярнрсть формы $(c^2-x^2)^{-\gamma}$, где $2c$ ширина диска и $0 \quad \gamma \cdot \frac{1}{2}$. Даётся ряд числовых примеров с краевыми трещинами или без них, под влиянием симметрической иди антисемметрической внешней нагрузки. Затем, рассматривается задача кручения, а именно, задача двух полубесконечных полос, под влиянием анти-плоской нагрузки сдвига. Вновь, даются результаты ряда числовых примеров с целью указания эффекта геометрии и свойств материала на фактор интенсивности напряжений.